AIMS Mathematics

http://www.aimspress.com/journal/Math

AIMS Mathematics, 5(1): 467–481.
DOI:10.3934/math.2020031
Received: 04 September 2019
Accepted: 28 November 2019
Published: 06 December 2019

Research article

Fractional physical problems including wind-influenced projectile motion with Mittag-Leffler kernel

Ramazan Ozarslan[1,*], **Erdal Bas**[1], **Dumitru Baleanu**[2,3] **and Bahar Acay**[1]

[1] Department of Mathematics, Science Faculty, Firat University, 23119 Elazig, Turkey
[2] Department of Mathematics and Computer Sciences, Faculty of Arts and Sciences, Cankaya University, Ankara, Turkey
[3] Institute of Space Sciences, Magurele-Bucharest, Romania

* **Correspondence:** Email: ozarslanramazan@gmail.com.

Abstract: In this manuscript the fractional form of wind-influenced projectile motion equations which have a significant place in physics is extensively investigated by preserving dimensionality of the physical quantities for fractional operators and features of wind-influenced projectile motion are computed analytically in view of Atangana-Baleanu (ABC) fractional derivative in Caputo sense. Moreover, ABC fractional derivative with $(n+\alpha)$th-order and its Laplace transform (LT) are obtained, $\alpha \in [0,1]$ and $n \in \mathbb{N}$. A comparative analysis based on the classical case is carried out in order to shed more light on the potent of the ABC fractional operator. Hence we present the results for some values of α, k friction constant, different wind effects and different masses in 3D illustrations by comparing Caputo fractional operator. Thus, we can observe trajectory, time of flight, maximum height and range clearly. Moreover, the obtained results are shown to correspond to the classical case while the order $\alpha \to 1$.

Keywords: projectile motion; fractional model; Atangana-Baleanu fractional derivative; wind; drag
Mathematics Subject Classification: 26A33, 97M50, 70E17

1. Introduction

The reason of increasing popularity of fractional calculus is the natural appearance of its applications in diverse areas of applied sciences and engineering. Fractional differential equations (FDEs) involving real or complex order derivatives have proven to be a useful tool in modelling anomalous dynamics of various physical and biological processes. One of the most important tasks for fractional operators is to apply them to real world phenomena and to see the differences between them. Using real data, Diethelm in [1] has presented a Caputo fractional model for better

understanding of the dynamics of a dengue fever outbreak. The authors in [2] have fractionalized a model in Caputo sense to get better dynamics of TB virus using real data whereas the dynamics of Ebola epidemic was better described in [3] using the Caputo fractional derivative. The fractional equivalent of various standard physics such as Schrödinger, frictional force, wave equation, harmonic oscillator, Dirac equation and projectile motion equation which all theoretical physics can be studied in via fractional calculus [4]. Chaotic systems, random walk problems, polymer material science and biophysics which are all applied physics and also be investigated by fractional calculus [5–13]. Furthermore, Bas et al., Yusuf et al. and Abdeljawad studied fractional derivatives in a different way in [14–18].

In nature, numerous physical features possess an intrinsic fractional order types [19, 20], for this reason fractional calculus has become so important instrument due to its efficiency in explaining real world phenomena more accurately. Fractional calculus stipulates a potent instrument for controlling memory and hereditary characteristics of several materials and processes [21]. This is one of the great significance of fractional calculus when compared with the ordinary calculus, whereas such control has no many effects. A lot of physical features have been analyzed via the concept of fractional calculus, with a very much amelioration over their integer order counterparts as well as more effective result when conferring with experimental data, i.e., in chemical, agricultural, biomedical, and also from physical perspectives such as Hamiltonian formulation and Lagrangian [22, 23]. Owing to this impressive usefulness of fractional calculus, a number of fractional operators have been proposed to precisely model the memory effects dealing with variety of dynamical systems [24–27]. However, more works need to be done to properly expound such dynamical systems. Riemann-Liouville and Caputo are some of the well-known fractional derivatives with the limitations of kernels with the singular structure. It can be easily seen that these derivatives can not properly depict the whole of memory effect of a particular system. To expunge this deficit of kernel with singular nature, the authors in [28, 29] introduced a fractional operator founded on the exponential and Mittag-Leffler functions, and thus, their definitions do not contain kernel of singular nature.

In light of the significance of the ABC fractional operator in engineering, science and in depicting the entire memory effect of the system, we feel motivated to investigate and analyze the projectile motion equations by means of ABC fractional derivative. Authors in [30–36] also studied fractional version of projectile motion. One of the most important problems in the field of physics is the projectile motion in a resistant medium. Furthermore, interesting structures of the projectile motion under wind effect are analyzed in [37].

It is known that the projectile motion has a movement with 2-dimension. Herein, we discuss such associated wind-influenced projectile motion. Projectile motion can be regarded as the movement of a launched object under gravitational force and symbols used are given by g with m/s^2, mass m with kg and unheeding any of the corresponding external or resisting force k with s^{-1}. Surmising that the particle begins at origin that is to say at ($x_0 = y_0 = 0\ m$), containing initial velocity with an angle ϕ, θ is the angle the wind makes with respect to the horizontal axis x, $U\ m/s$ is the wind speed, and modulus $v_0\ m/s$, then, in xy-plane one can present the classical equations of wind-influenced projectile motion [37] as

$$m\frac{dv_x}{dt} = -k(v_x - U\cos\theta), \quad m\frac{dv_y}{dt} = -mg - k(v_y - U\sin\theta), \tag{1.1}$$

with the initial velocities of the projectile

$$v_{0x} = v_0 \cos\phi, \tag{1.2}$$

$$v_{0y} = v_0 \sin\phi. \tag{1.3}$$

The corresponding solutions of (1.1)-(1.2) and (1.1)-(1.3) can be presented as,

$$x(t) = \frac{m}{k}(v_{0x} - U\cos\theta)\left(1 - e^{-\frac{kt}{m}}\right) + (U\cos\theta)t, \tag{1.4}$$

$$y(t) = \frac{m}{k}(\frac{mg}{k} - U\sin\theta + v_{0y})\left(1 - e^{-\frac{kt}{m}}\right) - (\frac{mg}{k} - U\sin\theta)t. \tag{1.5}$$

The manuscript has been prepared as follows: In section 2, essential definitions, properties and theorems associated with ABC fractional operator are presented. In section 3, $(n+\alpha)$th-order ABC operator is identified and its Laplace transform (LT) is proved for solving higher order linear initial value problems with Mittag-Leffler kernel when $\alpha \in [0,1]$ and $n \in \mathbb{N}$. In section 4, we present some numerical results and compare obtained results with ABC and Caputo fractional derivatives for different values of α and k friction coefficients, different wind effects and different masses in 3D illustration. Finally, some conclusion comments are given in section 5.

2. Preliminaries

In here we provide some important definitions, properties and theorems that will serve as a tool to the main results of the manuscript.

Definition 2.1. *[38] The Atangana-Baleanu left and right fractional derivatives in Caputo form involving Mittag-Leffler function are given by*

$${}^{ABC}_{a}D^{\alpha} f(t) = \frac{B(\alpha)}{1-\alpha}\int_a^t f'(s)E_\alpha\left(\frac{-\alpha}{1-\alpha}(t-s)^\alpha\right)ds, \tag{2.1}$$

$${}^{ABC}D^{\alpha}_{b} f(t) = \frac{-B(\alpha)}{1-\alpha}\int_t^b f'(s)E_\alpha\left(\frac{-\alpha}{1-\alpha}(s-t)^\alpha\right)ds, \tag{2.2}$$

where $f \in H^1(a,b), a < b, \alpha \in [0,1]$ and $B(\alpha)$ is a normalization function that satisfy $B(\alpha) > 0$, $B(0) = B(1) = 1$.

Theorem 2.1. *[38] ABC derivative has the following LT, $0 < \alpha \leq 1$,*

$$\mathcal{L}\{{}^{ABC}_{a}D^{\alpha} f(t)\}(s) = \frac{B(\alpha)}{1-\alpha}\frac{s^\alpha \mathcal{L}\{f(t)\}(s) - s^{\alpha-1}f(a)}{s^\alpha + \frac{\alpha}{1-\alpha}}. \tag{2.3}$$

Definition 2.2. *[39] Mittag-Leffler function is expressed as*

$$E_\alpha(x) = \sum_{k=0}^{\infty}\frac{x^k}{\Gamma(\alpha k+1)},\ \alpha > 0, \tag{2.4}$$

$$E_{\alpha,\beta}(x) = \sum_{k=0}^{\infty}\frac{x^k}{\Gamma(\alpha k+\beta)},\ \alpha,\beta > 0. \tag{2.5}$$

Definition 2.3. *[39] For $\alpha \in [n-1, n)$, the Caputo fractional derivative is defined as*

$$ {}_a^C D^{\alpha}(f)(t) = \frac{1}{\Gamma(n-\alpha)} \int_0^t \left[\frac{f^{(n)}(x)}{(t-x)^{\alpha-n+1}} \right] dx. \tag{2.6} $$

Theorem 2.2. *[40] The Laplace transform of Caputo fractional derivative is given by*

$$ \mathcal{L}\{{}_0^C D_t^{\alpha} f(t)\} = s^{\alpha} f(s) - \sum_{k=0}^{n-1} s^{\alpha-k-1} f^{(k)}(0). $$

Definition 2.4. *[40] Let $f, g : [0, \infty) \to \mathbb{R}$ and their convolution can be expressed as*

$$ (f * g)(t) = \int_0^t f(s) g(t-s) ds. \tag{2.7} $$

Property 2.1. [40] The LT has the following property,

$$ \mathcal{L}\{(f * g)(t)\} = \mathcal{L}\{f(t)\}\mathcal{L}\{g(t)\}. \tag{2.8} $$

Property 2.2. [40] The inverse LT of some specific functions as below:

i) $\mathcal{L}^{-1}\left\{ \frac{s^{\alpha}}{s(s^{\alpha}+a)} \right\} = E_{\alpha}(-at^{\alpha})$.

ii) $\mathcal{L}^{-1}\left\{ \frac{a}{s(s^{\alpha}+a)} \right\} = 1 - E_{\alpha}(-at^{\alpha})$.

iii) $\mathcal{L}^{-1}\left\{ \frac{1}{(s^{\alpha}+a)} \right\} = t^{\alpha-1} E_{\alpha,\alpha}(-at^{\alpha})$.

3. Main results

In this portion, the main findings and results of the paper such as definition of ABC fractional derivative with $(n+\alpha)th$-order and its corresponding Laplace transform, projectile motion in a resistant medium with ABC fractional derivative will be presented.

Definition 3.1. *Let $0 < \alpha \leq 1$, the definition of ABC fractional derivative with $(n+\alpha)th$-order is defined as following formula*

$$ {}^{ABC}_{a}D^{(\alpha+n)} f(t) = \frac{B(\alpha)}{1-\alpha} \int_a^t f^{(n+1)}(s) E_{\alpha}\left[\frac{-\alpha}{1-\alpha}(t-s)^{\alpha} \right] ds, \;\; 0 < \alpha \leq 1, n \in \mathbb{N}. \tag{3.1} $$

Theorem 3.1. *If $f(t)$ satisfies equation (3.1), then the LT of (3.1) is as following equality,*

$$ \mathcal{L}\{{}^{ABC}_{a}D^{(\alpha+n)} f(t)\}(s) = \frac{B(\alpha)}{1-\alpha} \frac{[s^{n+1}\mathcal{L}\{f(t)\} - \sum_{k=0}^{n} s^{\alpha+n-k-1} f^{(k)}(a)]}{s^{\alpha} + \frac{\alpha}{1-\alpha}}. \tag{3.2} $$

Proof. Let $0 < \alpha \leq 1$, taking the LT of both sides of (3.1) and performing necessary operations,

$$\begin{aligned}
\mathcal{L}\{{}^{ABC}_{a}D^{(\alpha+n)}f(t)\} &= \frac{B(\alpha)}{1-\alpha}\mathcal{L}\{f^{(n+1)}(t)\}\mathcal{L}\left\{E_\alpha\left(\frac{-\alpha}{1-\alpha}t^\alpha\right)\right\} \\
&= \frac{B(\alpha)}{1-\alpha}\left[s^{n+1}\mathcal{L}\{f(t)\} - s^n f(a) - s^{n-1}f(a) - \cdots - f^{(n)}(a)\right]\frac{s^{\alpha-1}}{s^\alpha + \frac{\alpha}{1-\alpha}} \\
&= \frac{B(\alpha)}{1-\alpha}\frac{[s^{n+\alpha}\mathcal{L}\{f(t)\} - \sum_{k=0}^{n} s^{\alpha+n-k-1}f^{(k)}(a)]}{s^\alpha + \frac{\alpha}{1-\alpha}},
\end{aligned} \tag{3.3}$$

thus, last equation is obtained and this completes the proof. □

3.1. Wind-influenced fractional projectile motion with Mittag-Leffler kernel

There exist some resistances from the practical point of view whose effects can be modelled with fractional operators and a drag force. To this aim, we utilize ABC fractional operator to model projectile motion equations under wind effect. We consequently obtain some novel exact expressions for this equation.

At first, let us give the fractional form of ordinary derivative

$$\frac{d}{dt} \to K^{1-\alpha}\,{}^{ABC}_{a}D^{\alpha}, \tag{3.4}$$

where K is a dimension (s^{-1}). Starting from this, we can give the fractional version of (1.1) in the ABC sense

$$mK^{1-\alpha}\,{}^{ABC}_{a}D^{\alpha}v_x(t) = -k(v_x(t) - U\cos\theta) \tag{3.5}$$

$$mK^{1-\alpha}\,{}^{ABC}_{a}D^{\alpha}v_y(t) = -k(v_y(t) - U\sin\theta) - mg \tag{3.6}$$

with the initial conditions

$$v_{0x} = v_0\cos\phi \tag{3.7}$$

$$v_{0y} = v_0\sin\phi \tag{3.8}$$

Taking the LT of both sides of (3.5), we have

$$\mathcal{L}\{mK^{1-\alpha}\,{}^{ABC}_{a}D^{\alpha}v_x(t)\} = \mathcal{L}\{-k(v_x(t) - U\cos\theta)\}, \tag{3.9}$$

thus one can attain

$$mK^{1-\alpha}\frac{B(\alpha)}{1-\alpha}\frac{s^\alpha\mathcal{L}\{v_x(t)\} - s^{\alpha-1}v_x(0)}{s^\alpha + \frac{\alpha}{1-\alpha}} = \mathcal{L}\{-k(v_x(t) - U\cos\theta)\}, \tag{3.10}$$

and this yields

$$\begin{aligned}
v_x(t) &= \frac{B(\alpha)\,mK^{1-\alpha}v_0\cos\phi + kU\cos\theta(1-\alpha)}{B(\alpha)\,mK^{1-\alpha} + k(1-\alpha)}E_\alpha\left(\frac{-k\alpha}{B(\alpha)\,mK^{1-\alpha} + k(1-\alpha)}t^\alpha\right) \\
&\quad + U\cos\theta\left(1 - E_\alpha\left(\frac{-k\alpha}{B(\alpha)\,mK^{1-\alpha} + k(1-\alpha)}t^\alpha\right)\right),
\end{aligned} \tag{3.11}$$

where $B(\alpha)$ is a normalization constant such that $B(0) = B(1) = 1$. If we use formula (3.2), we have

$$\begin{aligned} x(t) &= \frac{B(\alpha)\, mK^{1-\alpha}v_0 \cos\phi + kU\cos\theta\,(1-\alpha)}{B(\alpha)\, mK^{1-\alpha} + k\,(1-\alpha)} tE_{\alpha,2}\left(\frac{-k\alpha}{B(\alpha)\, mK^{1-\alpha} + k\,(1-\alpha)}t^{\alpha}\right) \\ &\quad + Ut\cos\theta\left(1 - E_{\alpha,2}\left(\frac{-k\alpha}{B(\alpha)\, mK^{1-\alpha} + k\,(1-\alpha)}t^{\alpha}\right)\right). \end{aligned} \tag{3.12}$$

Performing similar operations to the equation (3.6), we have

$$\begin{aligned} v_y(t) &= \frac{B(\alpha)\, mK^{1-\alpha}v_0 \sin\phi + (kU\sin\theta - mg)\,(1-\alpha)}{B(\alpha)\, mK^{1-\alpha} + k\,(1-\alpha)} E_{\alpha}\left(\frac{-k\alpha}{B(\alpha)\, mK^{1-\alpha} + k\,(1-\alpha)}t^{\alpha}\right) \\ &\quad + \frac{(kU\sin\theta - mg)}{k}\left(1 - E_{\alpha}\left(\frac{-k\alpha}{B(\alpha)\, mK^{1-\alpha} + k\,(1-\alpha)}t^{\alpha}\right)\right). \end{aligned} \tag{3.13}$$

$$\begin{aligned} y(t) &= \frac{B(\alpha)\, mK^{1-\alpha}v_0 \sin\phi + (kU\sin\theta - mg)\,(1-\alpha)}{B(\alpha)\, mK^{1-\alpha} + k\,(1-\alpha)} tE_{\alpha,2}\left(\frac{-k\alpha}{B(\alpha)\, mK^{1-\alpha} + k\,(1-\alpha)}t^{\alpha}\right) \\ &\quad + \frac{(kU\sin\theta - mg)\,t}{k}\left(1 - E_{\alpha,2}\left(\frac{-k\alpha}{B(\alpha)\, mK^{1-\alpha} + k\,(1-\alpha)}t^{\alpha}\right)\right). \end{aligned} \tag{3.14}$$

Note that the results obtained above (1.4) can be found for all classical cases while the order $\alpha \to 1$. Moreover one can obtain flight time T from $y(T) = 0$,

$$\begin{aligned} y(T) &= \frac{B(\alpha)\, mK^{1-\alpha}v_0 \sin\phi + (kU\sin\theta - mg)\,(1-\alpha)}{B(\alpha)\, mK^{1-\alpha} + k\,(1-\alpha)} TE_{\alpha,2}\left(\frac{-k\alpha}{B(\alpha)\, mK^{1-\alpha} + k\,(1-\alpha)}T^{\alpha}\right) \\ &\quad + \frac{(kU\sin\theta - mg)\,T}{k}\left(1 - E_{\alpha,2}\left(\frac{-k\alpha}{B(\alpha)\, mK^{1-\alpha} + k\,(1-\alpha)}T^{\alpha}\right)\right) \\ &= 0. \end{aligned}$$

We can calculate it for approximate value of Mittag-Leffler function

$$\begin{aligned} &\frac{B(\alpha)\, mK^{1-\alpha}v_0 \sin\phi + (kU\sin\theta - mg)\,(1-\alpha)}{B(\alpha)\, mK^{1-\alpha} + k\,(1-\alpha)} T\sum_{i=0}^{\infty}\frac{\left(\frac{-k\alpha}{B(\alpha)mK^{1-\alpha}+k(1-\alpha)}T^{\alpha}\right)^{i}}{\Gamma[i\alpha+2]} \\ &\qquad + \frac{(kU\sin\theta - mg)\,T}{k}\left(1 - \sum_{i=0}^{\infty}\frac{\left(\frac{-k\alpha}{B(\alpha)mK^{1-\alpha}+k(1-\alpha)}T^{\alpha}\right)^{i}}{\Gamma[i\alpha+2]}\right) = 0, \end{aligned}$$

from here similarly range R can be calculated from $x(T) = R$ for the approximate value of Mittag-Leffler function.

3.2. Wind-influenced fractional projectile motion with singular kernel

Now, let's apply Caputo fractional operator to model projectile motion equations under wind effect.

$$mK^{1-\alpha}{}_{a}^{C}D^{\alpha}v_y(t) = -k(v_y(t) - U\sin\theta) - mg, \tag{3.15}$$

$$mK^{1-\alpha}{}_{a}^{C}D^{\alpha}v_x(t) = -k(v_x(t) - U\cos\theta). \tag{3.16}$$

Taking the LT of both sides of (3.15) and (3.16) with the initial conditions (3.7)-(3.8) by Theorem (2.2), and subsequently applying inverse LT we have vertical and horizontal displacements and velocities

$$v_x(t) = v_0 \cos\phi E_\alpha\left(\frac{-k}{mK^{1-\alpha}}t^\alpha\right) + U\cos\theta\left(1 - E_\alpha\left(\frac{-k}{mK^{1-\alpha}}t^\alpha\right)\right), \tag{3.17}$$

$$x(t) = v_0 t\cos\phi E_{\alpha,2}\left(\frac{-k}{mK^{1-\alpha}}t^\alpha\right) + Ut\cos\theta\left(1 - E_{\alpha,2}\left(\frac{-k}{mK^{1-\alpha}}t^\alpha\right)\right), \tag{3.18}$$

$$v_y(t) = v_0 \sin\phi E_\alpha\left(\frac{-k}{mK^{1-\alpha}}t^\alpha\right) + \frac{kU\sin\theta - mg}{k}\left(1 - E_\alpha\left(\frac{-k}{mK^{1-\alpha}}t^\alpha\right)\right), \tag{3.19}$$

$$y(t) = v_0 t\sin\phi E_{\alpha,2}\left(\frac{-k}{mK^{1-\alpha}}t^\alpha\right) + \frac{kU\sin\theta - mg}{k}t\left(1 - E_{\alpha,2}\left(\frac{-k}{mK^{1-\alpha}}t^\alpha\right)\right). \tag{3.20}$$

Following the same procedure for wind-influenced projectile motion with ABC fractional derivative,we can find range and time of flight for the equations (3.15) and (3.16).

Note that, from the above obtained results, the results for classical cases represented in Eqs. (1.4) and (1.5) can be obtained for the projectile motion in resistive medium by taking limit $\alpha \to 1$.

4. Numerical discussion

In the portion, we provide the physical features and performances of the underlying wind-influenced projectile equations involving ABC and Caputo fractional operators. We suppose $K = k$ and $B(\alpha) = 1$ in our results. We illustrate the governing wind-influenced projectile motion equation with fractional ABC derivative with the order $(\alpha + 1)$ and under different α orders, different initial velocities, different air drags, different wind effects and different angles in 3-D figures. θ is the angle the wind makes with respect to the horizontal axis x, U m/s is the wind speed, $U = 0$ shows no-wind position, and t is the time (second).

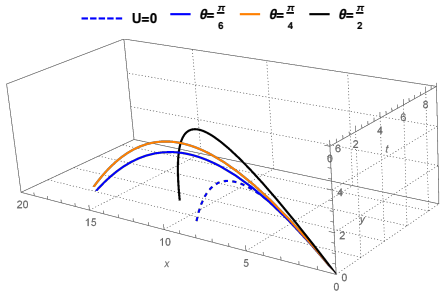

Figure 1. Comparative analysis of projectile motion under different wind angles, $v_0 = 22m/s, k = 0.01s^{-1}, m = 0.01kg, g = 9.8m/s^2, \phi = \frac{\pi}{4}, U = 5m/s, \alpha = 0.9$.

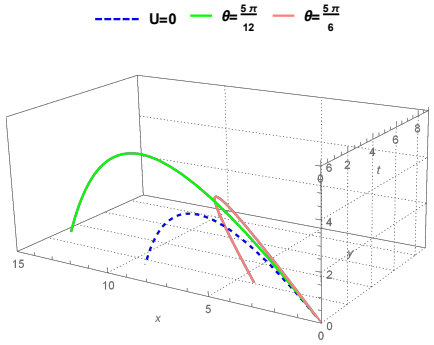

Figure 2. Comparative analysis of projectile motion under different wind angles, $v_0 = 22m/s, k = 0.01s^{-1}, m = 0.01kg, g = 9.8m/s^2, \phi = \frac{\pi}{4}, U = 5m/s, \alpha = 0.9$.

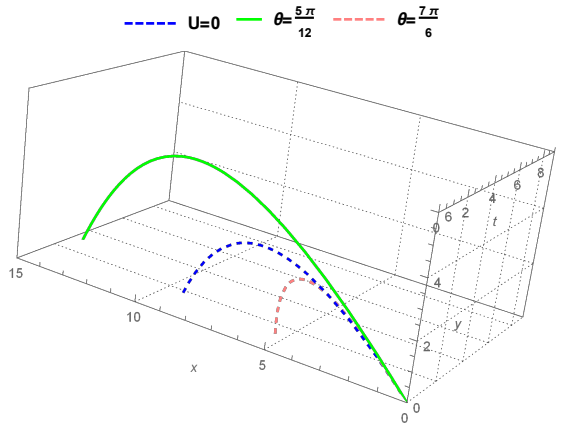

Figure 3. Comparative analysis of projectile motion under different wind angles, $v_0 = 22m/s, k = 0.01s^{-1}, m = 0.01kg, g = 9.8m/s^2, \phi = \frac{\pi}{4}, U = 5m/s, \alpha = 0.9$.

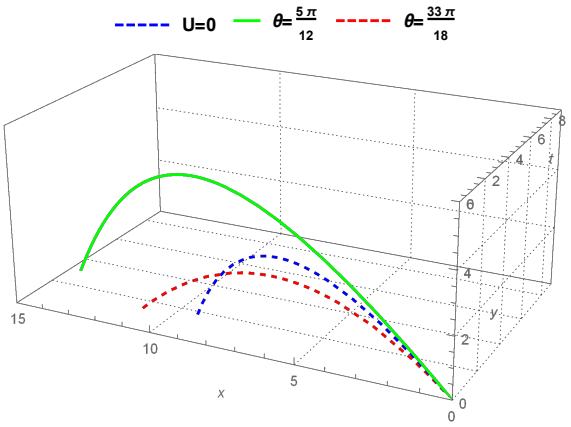

Figure 4. Comparative analysis of projectile motion under different wind angles, $v_0 = 22m/s, k = 0.01s^{-1}, m = 0.01kg, g = 9.8m/s^2, \phi = \frac{\pi}{4}, U = 5m/s, \alpha = 0.9$.

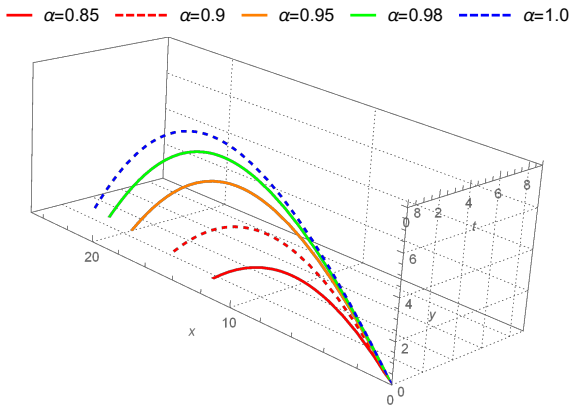

Figure 5. Comparative analysis of wind-influenced projectile motion under different fractional orders, $v_0 = 22m/s, k = 0.01s^{-1}, m = 0.01kg, g = 9.8m/s^2, \phi = \frac{\pi}{6}, \theta = \frac{\pi}{3}, U = 5m/s$.

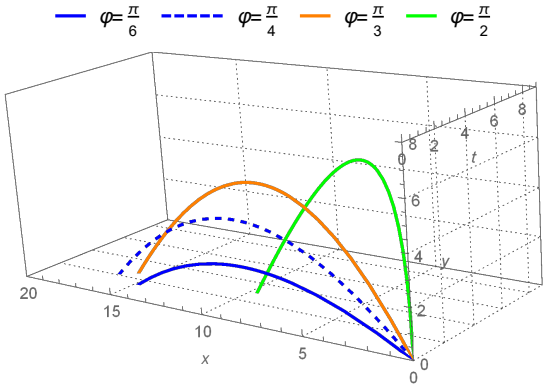

Figure 6. Comparative analysis of wind-influenced projectile motion under different launch angles, $v_0 = 22m/s, k = 0.01s^{-1}, m = 0.01kg, g = 9.8m/s^2, \theta = \frac{\pi}{3}, U = 5m/s$.

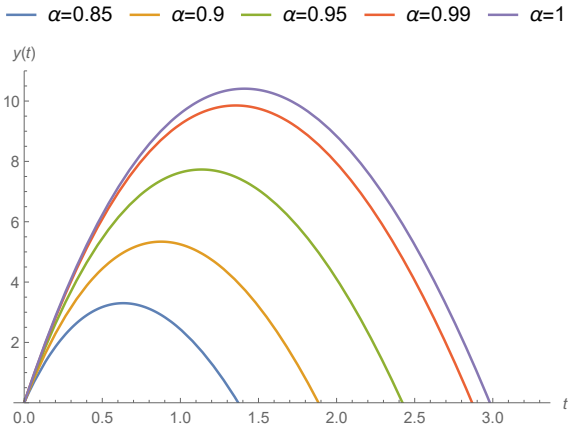

Figure 7. Comparative analysis of wind-influenced projectile motion for vertical displacement under different fractional orders, $v_0 = 22m/s, k = 0.01s^{-1}, m = 0.045kg, g = 9.8m/s^2, \phi = \frac{\pi}{4}, \theta = \frac{\pi}{3}, U = 2m/s$.

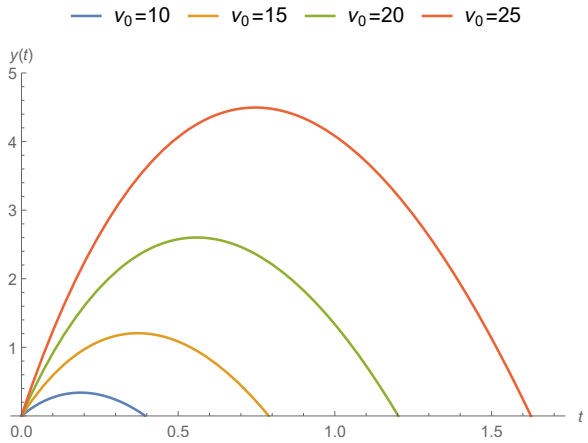

Figure 8. Comparative analysis of wind-influenced projectile motion for vertical displacement under different launch velocities, $\alpha = 0.85, k = 0.01s^{-1}, m = 0.045kg, g = 9.8m/s^2, \phi = \frac{\pi}{4}, \theta = \frac{\pi}{3}, U = 2m/s$.

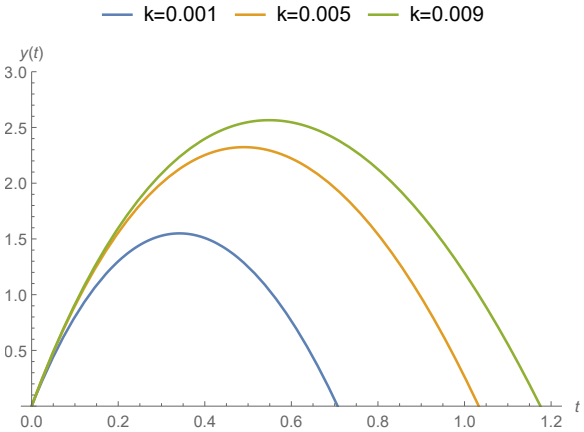

Figure 9. Comparative analysis of wind-influenced projectile motion for vertical displacement under different drag forces, $\alpha = 0.85, v_0 = 20m/s, m = 0.045kg, g = 9.8m/s^2, \phi = \frac{\pi}{4}, \theta = \frac{\pi}{3}, U = 2m/s$.

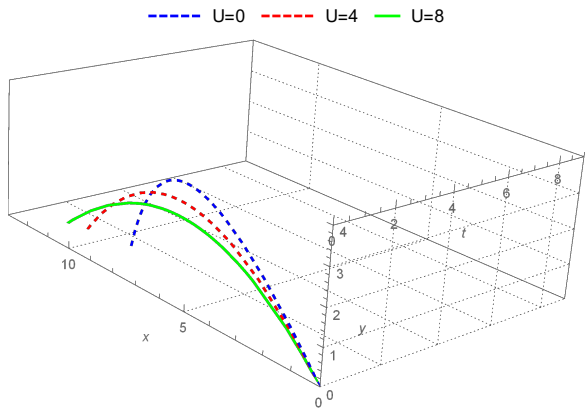

Figure 10. Comparative analysis of wind-influenced projectile motion under different wind speeds, $\alpha = 0.9, v_0 = 22m/s, m = 0.01kg, k = 0.01s^{-1}, g = 9.8m/s^2, \phi = \frac{\pi}{4}, \theta = \frac{33\pi}{18}$.

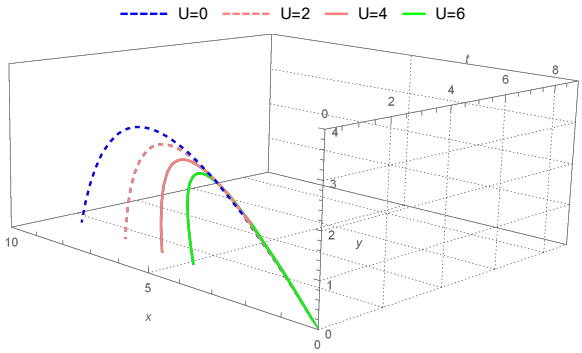

Figure 11. Comparative analysis of wind-influenced projectile motion under different wind speeds, $\alpha = 0.9, v_0 = 22m/s, m = 0.01kg, k = 0.01s^{-1}, g = 9.8m/s^2, \phi = \frac{\pi}{4}, \theta = \frac{7\pi}{6}$.

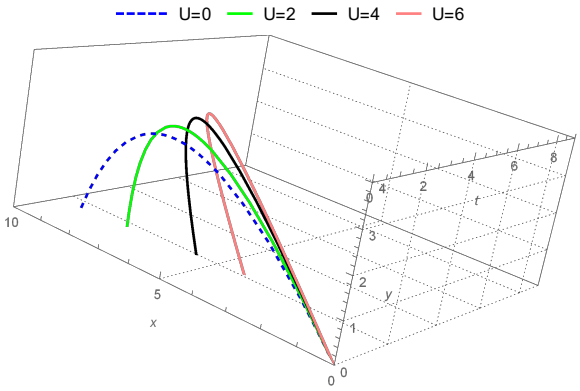

Figure 12. Comparative analysis of wind-influenced projectile motion under different wind speeds, $\alpha = 0.9, v_0 = 22m/s, m = 0.01kg, k = 0.01s^{-1}, g = 9.8m/s^2, \phi = \frac{\pi}{4}, \theta = \frac{5\pi}{6}$.

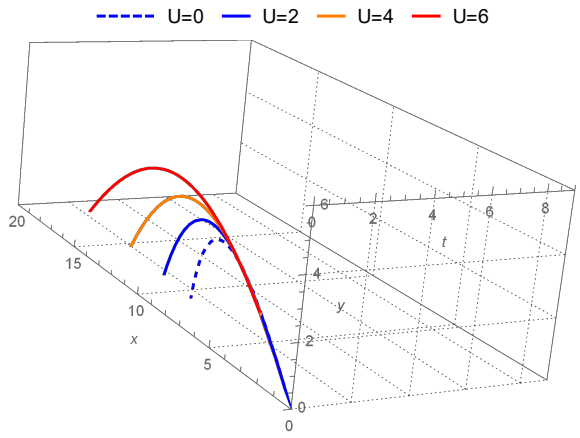

Figure 13. Comparative analysis of wind-influenced projectile motion under different wind speeds, $\alpha = 0.9, v_0 = 22m/s, m = 0.01kg, k = 0.01s^{-1}, g = 9.8m/s^2, \phi = \frac{\pi}{4}, \theta = \frac{\pi}{6}$.

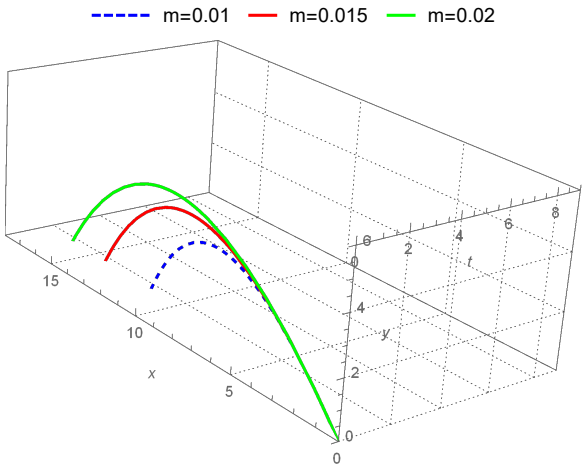

Figure 14. Comparative analysis of wind-influenced projectile motion under different masses, $\alpha = 0.9, v_0 = 22m/s, k = 0.01s^{-1}, g = 9.8m/s^2, \phi = \frac{\pi}{4}, \theta = \frac{\pi}{6}, U = 2m/s$.

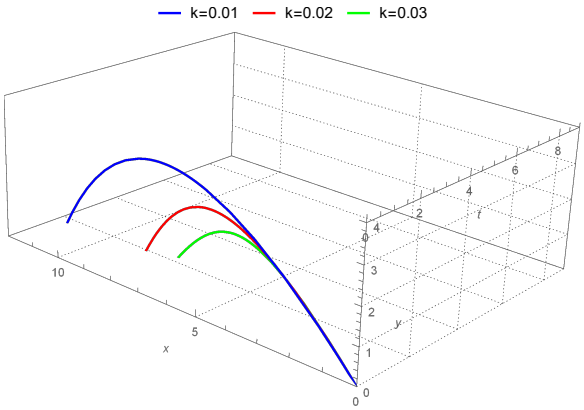

Figure 15. Comparative analysis of wind-influenced projectile motion under different drag forces $\alpha = 0.9, v_0 = 22m/s, m = 0.01kg, g = 9.8m/s^2, \phi = \frac{\pi}{4}, \theta = \frac{\pi}{6}, U = 2m/s.$

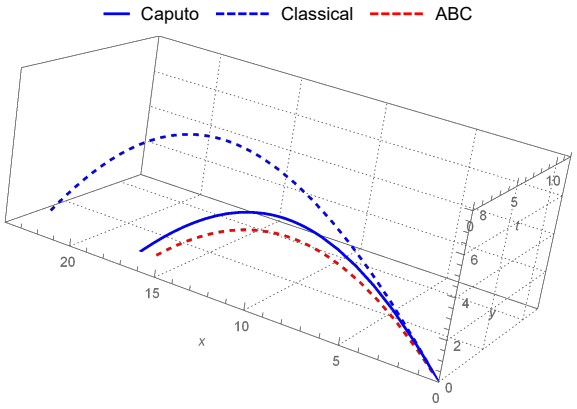

Figure 16. Comparative analysis of wind-influenced projectile motion with ABC, classical and Caputo fractional derivatives $\alpha = 0.9, v_0 = 22m/s, m = 0.01kg, g = 9.8m/s^2, \phi = \frac{\pi}{4}, \theta = \frac{\pi}{3}, U = 5m/s.$

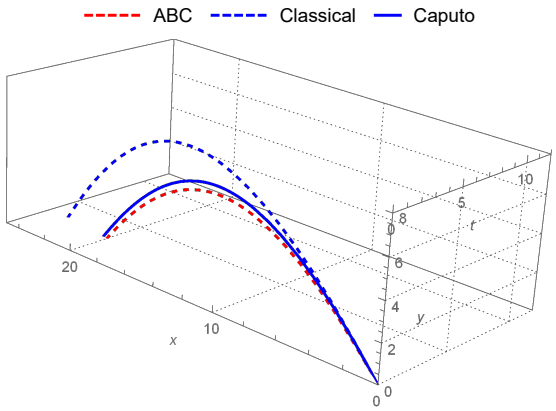

Figure 17. Comparative analysis of wind-influenced projectile motion with ABC, classical and Caputo fractional derivatives $\alpha = 0.95, v_0 = 22m/s, m = 0.01kg, g = 9.8m/s^2, \phi = \frac{\pi}{4}, \theta = \frac{\pi}{3}, U = 5m/s.$

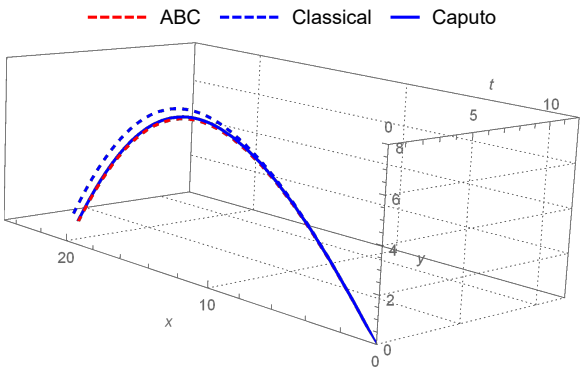

Figure 18. Comparative analysis of wind-influenced projectile motion with ABC, classical and Caputo fractional derivatives $\alpha = 0.99, v_0 = 22m/s, m = 0.01kg, g = 9.8m/s^2, \phi = \frac{\pi}{4}, \theta = \frac{\pi}{3}, U = 5m/s.$

5. Conclusions

We have studied wind-influenced projectile motion via ABC fractional derivative and have presented projectile motion equations in wind influenced medium with the aid of Laplace transform of ABC fractional operator. Due to the advantages of ABC fractional derivative, we have used this fractional derivative for wind-influenced projectile motion with air drag. It is well-known that preserving the dimensionality in physical quantities has so significance and so it has been preserved in this study. Moreover, we have expressed $(n + \alpha)$th-order ABC fractional derivative and demonstrate its Laplace transform. The attained results via fractional operators are close with that of the classical versions. We illustrate wind-influenced projectile motion with ABC-fractional derivative under different wind effects, different angles, different orders, different velocities, different masses and air drags in 3-D figures.

From Figure 7 and Figure 5, it is evident that the fractional parameter α serves as the resisting parameter and resistivity of the medium varies inversely with the increasing values of the fractional parameter, so for small value of alpha height as well as the range of the projectile is least.

- Figure 1 shows the effect of tailwind on the projectile motion under different wind angles between $[0, \frac{\pi}{2}]$ and so the particle moves forward. We observe that if the wind effects with $\theta = \frac{\pi}{4}$, range will be maximum and if the wind effects with $\theta = \frac{\pi}{2}$, range will be minimum relative to the other wind effects and it will reach to maximum height.
- Figures 2 and 3 show the effect of headwind on the projectile motion under different wind angles between $(\frac{\pi}{2}, \frac{3\pi}{2})$. We observe that if the wind effects with $\theta = \frac{5\pi}{6}$, the particle moves backward, and max-height increases. If the wind effects with $\theta = \frac{7\pi}{6}$, the particle moves backward, and max-height decreases.
- Figure 4 shows the effect of headwind on the projectile motion under different wind angles between $(\frac{3\pi}{2}, 2\pi)$ and so the particle moves forward. We observe that if the wind effects with $\theta = \frac{33\pi}{18}$, range decreases and max-height decreases.
- Figure 5 shows the effect of headwind on the projectile motion under different fractional orders with $\theta = \frac{\pi}{3}$, so the particle moves forward and max-height increases as the order increases. If the wind angle was headwind, then it would move backward.
- Figure 6 shows the effect of headwind on the projectile motion under different launch angles. We observe that time of flight and max-height increase as the angle increases. The particle reaches max range in $\phi = \frac{\pi}{4}$ and reaches max-height in $\phi = \frac{\pi}{2}$.
- Figures 7, 8, 9 show the effect of headwind on the projectile motion under different orders, launch velocities and masses for vertical displacement.
- Figure 10 shows the effect of tailwind on the projectile motion under different wind speeds while $\theta = \frac{33\pi}{18}$, so the particle moves forward and max-height decreases as the velocity increases.
- Figure 11 shows the effect of headwind on the projectile motion under different wind speeds while $\theta = \frac{7\pi}{6}$, so the particle moves backward and max-height decreases as the velocity increases.
- Figure 12 shows the effect of headwind on the projectile motion under different wind speeds while $\theta = \frac{5\pi}{6}$, so the particle moves backward and max-height increases as the velocity increases.
- Figure 13 shows the effect of tailwind on the projectile motion under different wind speeds while $\theta = \frac{\pi}{6}$, so the particle moves forward and max-height increases as the velocity increases.
- Figure 14 shows the effect of mass on the projectile motion while $\theta = \frac{\pi}{6}, \phi = \frac{\pi}{4}$, and we observe

that the particle moves forward, max-height increases as the mass increases.

- Figure 15 shows the effect of drag force on the projectile motion while $\theta = \frac{\pi}{6}, \phi = \frac{\pi}{4}$, and we observe that range and max-height increase as drag force decreases.
- Figures 16, 17, and 18 show the comparison of wind-influenced projectile motion with ABC, Caputo and classical cases while $\alpha \to 1$, and trajectories obtained by ABC and Caputo tend to converge to the trajectories by classical derivatives as $\alpha \to 1$.

Conflict of interest

The authors declare no conflict of interest in this paper.

References

1. K. Diethelm, *A fractional calculus based model for the simulation of an outbreak of dengue fever*, Nonlinear Dynam., **71** (2013), 613–619.
2. S. Ullah, M. A. Khan and M. Farooq, *A fractional model for the dynamics of TB virus*, Chaos Soliton. Fract., **116** (2018), 63–71.
3. I. Area, H. Batarfi, J. Losada, et al. *On a fractional order Ebola epidemic model*, Advances in Difference Equations, **2015** (2015), 278.
4. H. Richard, *Fractional calculus: an introduction for physicists*, World Scientific, 2014.
5. G. U. Varieschi, *Applications of Fractional Calculus to Newtonian Mechanics*, arXiv preprint arXiv:1712.03473, 2017.
6. M. H. Heydari, *Chebyshev cardinal functions for a new class of nonlinear optimal control problems generated by Atangana-Baleanu-Caputo variable-order fractional derivative*, Chaos Soliton. Fract., **130** (2020), 109401.
7. M. Hosseininia, M. H. Heydari, *Meshfree moving least squares method for nonlinear variable-order time fractional 2D telegraph equation involving Mittag–Leffler non-singular kernel*, Chaos Soliton. Fract., **127** (2019), 389–399.
8. M. Hosseininia, M. H. Heydari, *Legendre wavelets for the numerical solution of nonlinear variable-order time fractional 2D reaction-diffusion equation involving Mittag-Leffler non-singular kernel*, Chaos Soliton. Fract., **127** (2019), 400–407.
9. E. Bonyah, A. Atangana, A. A. Elsadany, *A fractional model for predator-prey with omnivore*, Chaos: An Interdisciplinary Journal of Nonlinear Science, **29** (2019), 013136.
10. A. Al-khedhairi, A. A. Elsadany, A. Elsonbaty, *Modelling immune systems based on Atangana–Baleanu fractional derivative*, Chaos Soliton. Fract., **129** (2019), 25–39.
11. M. A. Khan, A. Khan, A. Elsonbaty, et al. *Modeling and simulation results of a fractional dengue model*, The European Physical Journal Plus, **134** (2019), 379.
12. M. Yavuz, *Characterizations of two different fractional operators without singular kernel*, Math. Model. Nat. Pheno., **14** (2019), 302.

13. M. Goyal, H. M. Baskonus, A. Prakash, *An efficient technique for a time fractional model of lassa hemorrhagic fever spreading in pregnant women*, The European Physical Journal Plus, **134** (2019), 482.

14. T. Abdeljawad, *Fractional operators with boundary points dependent kernels and integration by parts*, Discrete Contin. Dyn. Syst. Ser. S, (2019), 351.

15. E. Bas, R. Ozarslan, D. Baleanu, et al. *Comparative simulations for solutions of fractional Sturm-Liouville problems with non-singular operators*, Advances in Difference Equations, **2018** (2018), 350.

16. A. Yusuf, M. Inc, A. I. Aliyu, et al. *Efficiency of the new fractional derivative with nonsingular Mittag-Leffler kernel to some nonlinear partial differential equations*, Chaos Soliton. Fract., **116** (2018), 220–226.

17. E. Bas, *The Inverse Nodal problem for the fractional diffusion equation*, Acta Scientiarum. Technology, **37** (2015), 251–257.

18. T. Abdeljawad, *A Lyapunov type inequality for fractional operators with nonsingular Mittag-Leffler kernel*, J. Inequal. Appl., **2017** (2017), 130.

19. M. Caputo, F. Mainardi, *A new dissipation model based on memory mechanism*, Pure Appl. Geophys., **91** (1971), 134–147.

20. R. L. Magin, O. Abdullah, D. Baleanu, et al. *Anomalous diffusion expressed through fractional order differential operators in the Bloch Torrey equation*, J. Magn. Reson., **190** (2008), 255–270.

21. V. V. Uchaikin, *Fractional derivatives for physicists and engineers*, Berlin: Springer, 2013.

22. R. L. Magin, *Fractional calculus in bioengineering*, Redding: Begell House, 2006.

23. A. K. Golmankhaneh, A. M. Yengejeh and D. Baleanu, *On the fractional Hamilton and Lagrange mechanics*, Int. J. Theor. Phys., **51** (2012), 2909–2916.

24. D. G. Prakasha, P. Veeresha, H. M. Baskonus, *Analysis of the dynamics of hepatitis E virus using the Atangana-Baleanu fractional derivative*, The European Physical Journal Plus, **134** (2019), 241.

25. W. Gao, B. Ghanbari, H. M. Baskonus, *New numerical simulations for some real world problems with Atangana–Baleanu fractional derivative*, Chaos Soliton. Fract., **128** (2019), 34–43.

26. M. Yavuz, N. Ozdemir, H. M. Baskonus, *Solutions of partial differential equations using the fractional operator involving Mittag-Leffler kernel*, The European Physical Journal Plus, **133** (2018), 215.

27. J. F. Gomez-Aguilar, J. J. Rosales-García, J. J. Bernal-Alvarado, et al. *Fractional mechanical oscillators*, Revista mexicana de física, **58** (2012), 348–352.

28. M. Caputo, M. Fabrizio, *A new definition of fractional derivative without singular kernel*, Progr. Fract. Differ. Appl, **1** (2015), 1–13.

29. A. Atangana and D. Baleanu, *New fractional derivatives with nonlocal and non-singular kernel: theory and application to heat transfer model*, Therm. Sci., **20** (2016), 757–763.

30. A. Ebaid, *Analysis of projectile motion in view of fractional calculus*, Appl. Math. Model., **35** (2011), 1231–1239.

31. A. O. Contreras, J. J. R. Garcia, L. M. Jimenez, et al. *Analysis of projectile motion in view of conformable derivative*, Open Phys., **16** (2018), 581–587.

32. B. Ahmad, H. Batarfi, J. J. Nieto, et al. *Projectile motion via Riemann-Liouville calculus*, Advances in Difference Equations, **2015** (2015), 63.

33. J. Losada, J. J. Nieto, *Properties of a new fractional derivative without singular kernel*, Progr. Fract. Differ. Appl, **1** (2015), 87–92.

34. J. Rosales, M. Guía, F. F. Gómez, et al. *Two dimensional fractional projectile motion in a resisting medium*, Open Phys., **12** (2014), 517–520.

35. F. M. Alharbi, D. Baleanu, A. Ebaid, *Physical properties of the projectile motion using the conformable derivative*, Chinese J. Phys., **58** (2019), 18–28.

36. J. F. Gomez-Aguilar, R. F. Escobar-Jiménez, M. G. Lopez-Lopez, et al. *Analysis of projectile motion: A comparative study using fractional operators with power law, exponential decay and Mittag-Leffler kernel*, The European Physical Journal Plus, **133** (2018), 103.

37. R. C. Bernardo, J. P. Esguerra, J. D. Vallejos, et al. *Wind-influenced projectile motion*, Eur. J. Phys., **36** (2015), 025016.

38. E. Bas, R. Ozarslan, *Real world applications of fractional models by Atangana-Baleanu fractional derivative*, Chaos Soliton. Fract., **116** (2018), 121–125.

39. I. Podlubny, *Fractional differential equations: an introduction to fractional derivatives, fractional differential equations, to methods of their solution and some of their applications*, Elsevier, 1998.

40. S. Liang, R. Wu, L. Chen, *Laplace transform of fractional order differential equations*, Electron. J. Differ. Equ., **2015** (2015), 1–15.

AIMS Press

© 2020 the Author(s), licensee AIMS Press. This is an open access article distributed under the terms of the Creative Commons Attribution License (http://creativecommons.org/licenses/by/4.0)